NASA

CCN-213

MEMORANDUM

CASE FILE COPY

PERFORMANCE OF AN AXISYMMETRIC EXTERNAL-COMPRESSION

AND A TWO-DIMENSIONAL EXTERNAL-INTERNAL-

COMPRESSION INLET AT MACH 4.95

By James F. Connors and Leverett A. Anderson, Jr.

Lewis Research Center
Cleveland, Ohio

NATIONAL AERONAUTICS AND SPACE ADMINISTRATION

WASHINGTON

February 1959

NATIONAL AERONAUTICS AND SPACE ADMINISTRATION

MEMORANDUM 12-18-58E

PERFORMANCE OF AN AXISYMMETRIC EXTERNAL-COMPRESSION

AND A TWO-DIMENSIONAL EXTERNAL-INTERNAL-

COMPRESSION INLET AT MACH 4.95 *

By James F. Connors and Leverett A. Anderson, Jr.

SUMMARY

An experimental evaluation was made of the performance of two different inlet configurations at a Mach number of 4.95. Both inlets incorporated some boundary-layer bleed in the vicinity of the throat and were designed for low cowl-lip drag.

An axisymmetric fixed-geometry external-compression inlet with a subsonic dump diffuser had a critical total-pressure recovery of 0.25 and a maximum recovery of 0.31 with corresponding mass-flow ratios of 0.93 and 0.74, respectively.

A two-dimensional external-internal-compression inlet attained a total-pressure recovery of 0.41 at a corresponding mass-flow ratio of 0.94. By means of its variable geometry, that is, a variable bypass door ahead of the throat, the inlet could be readily started.

INTRODUCTION

As flight speed is increased, the attainment of high internal performance becomes increasingly difficult and generally necessitates the use of variable-geometry features in the air-induction system. The achievement of such variable geometry becomes progressively more difficult because of the extreme temperature environments encountered. In the hypersonic regime, some method of cooling must be provided in order to maintain structural integrity. The dividing line between cooling and not cooling appears to lie somewhere around Mach 5.0 (see ref. 1). From a cooling viewpoint, of course, the simplicity of the fixed-geometry self-starting inlet is desirable. On the other hand, from the viewpoint of achieving high internal-flow performance, the merits of variable-geometry systems

---

*Title, Unclassified.

are also obvious in attaining large amounts of internal compression and superior off-design performance.

In the present study, an experimental evaluation was made of the internal performance of two representative inlets at a design Mach number of 4.95. These configurations consist of (1) a two-dimensional external-internal-compression inlet with a variable throat bypass (similar to the Mach 3.05 configuration of ref. 2) and (2) an axisymmetric external-compression inlet with a cylindrical cowl and a subsonic "dump" diffuser (similar to the Mach 3.85 configuration of ref. 3). Both inlets were designed for essentially zero cowl-lip drag. The experimental program was run at zero angle of attack and at a Reynolds number per foot of 5.7×10^6.

SYMBOLS

The following symbols are used in this report:

A_i maximum possible capture streamtube area, sq ft

M Mach number

m mass-flow rate, slugs/sec

m_0 maximum possible mass-flow rate, $\rho_0 A_i V_0$, slugs/sec

P total pressure, lb/sq ft

V velocity, ft/sec

x,y,z rectangular coordinates

γ ratio of specific heats for air

η_{KE} kinetic-energy efficiency defined as the ratio of kinetic energy available after diffusion (assuming isentropic reexpansion to ambient pressure) to the kinetic energy in the free stream,

$$1 - \frac{2}{(\gamma - 1)M_0^2} \left[\left(\frac{P_0}{P_3}\right)^{(\gamma-1)/\gamma} - 1 \right]$$

λ local flow direction relative to free-stream direction, deg

ρ density, slugs/ft^3

Subscripts:

0   free stream

1   throat station

3   diffuser-exit station

Superscript:

$-$ integrated average

APPARATUS AND PROCEDURE

The experimental investigation was conducted at a Mach number of 4.95 in a 1- by 1-foot wind tunnel at a Reynolds number per foot of 5.7×10^6. As schematically illustrated in figure 1(a), the axisymmetric model was sting mounted. The two-dimensional model (fig. 1(b)) was supported by two horizontal struts from the sides. In order to vary the inlet back pressure each model had a remotely controlled movable exit plug. The two-dimensional inlet was studied with sharp metal sideplates, swept back along the initial shock angle, and also with rectangular side-plates in which glass inserts were installed for internal-flow visualization with a twin-mirror schlieren apparatus.

The axisymmetric external-compression inlet (fig. 1(a)) had a contoured centerbody designed by the method of characteristics to turn the flow isentropically from an initial cone half-angle of 8° to a final half-angle of 32° at the diffuser entrance. Theoretically, this corresponded to compressing the flow from the free-stream Mach number of 4.95 down to a Mach number of 2.76. The resulting compression waves were calculated to be focused on the cowl lip. In order to achieve low drag, the inlet was designed with an internally cylindrical cowl. In the throat, a rearward-facing flush slot with a gap adjustable from zero to 0.25 inch was installed for boundary-layer control. Downstream of the throat, a subsonic "dump", or abrupt-area-discontinuity, diffuser (ref. 3) was installed (see fig. 1(d)). The area ratio between throat and diffuser exit was greater than would ordinarily be employed because existing model parts were used (ref. 3). As a result, the diffuser-exit Mach numbers were low, less than about 0.1. Theoretically, the maximum total-pressure recovery attainable with this type of inlet is 0.41 assuming only shock losses. This is reduced to 0.35 assuming a complete loss of the subsonic dynamic head due to dumping of the flow or merely a recovery of the static pressure behind a normal shock at the throat. Dimensional details of the spike and aft dump section are given in table I.

The aerodynamic design of the two-dimensional external-internal-compression inlet is shown by the theoretical shock patterns of figure 1(c). The design approach is the same as that used in reference 2. Isentropic compression focused at the cowl lip is produced by the external contoured ramp. Downstream of the lip a finite internal shock off the cowl turns the flow back to the free-stream direction. Again, isentropic focused compression is employed to turn the flow internally to a normal-shock Mach number in the throat of 1.8. With this compression scheme, the theoretical total-pressure recovery is 0.60 based solely on shock losses. During the course of the investigation, the external-ramp contour was modified in an attempt to reduce mass-flow spillage at the cowl lip. The change in coordinates are given in table II.

In order to start the inlet, that is, establish supersonic flow in the throat, a variable bypass door was installed on the external-compression ramp immediately ahead of the throat. The hinge point was located on a line drawn from the cowl lip perpendicular to the ramp surface. Starting was accomplished by opening the door and allowing large quantities of air to bypass the throat and be discharged to the external stream. Once supersonic flow was established, the door was returned to its design, or flush position. A flush-slot bleed system was located between the bypass door and the internal lip to control the ramp boundary layer before it was effected by the strong adverse pressure gradient of the internal-shock system. The subsonic diffuser was designed with a gradual over-all divergence rate, corresponding to an average 4° included angle. Dimensional details of the entire inlet are given in table II and photographs are shown in figure 1(e).

In the present study, total-pressure recovery was based on the area-weighted average of pitot tubes at the diffuser exit. Mass flow was computed from the measured static pressure at the diffuser exit and the calibrated sonic discharge area at the exit plug with the assumption of isentropic one-dimensional flow between the two stations.

RESULTS AND DISCUSSION

The experimental study at Mach 4.95 was made to determine the diffuser characteristics of two separate and distinct inlet geometries. The axisymmetric external-compression inlet is a fixed-geometry configuration and, as such, is limited both theoretically and experimentally to the attainment of pressure recoveries less than those for the two-dimensional inlet, which was designed with a high degree of internal compression and with the attendant complexity of variable geometry. Each inlet will be discussed separately.

Axisymmetric External-Compression Inlet

Diffuser performance characteristics at Mach 4.95 are presented in figure 2(a) for several settings of the boundary-layer bleed gap at the throat. With the best bleed arrangement (gap = 0.125 in.), a critical pressure recovery of about 0.25 was obtained at a mass-flow ratio of 0.93 and a peak recovery of 0.31 was obtained at a mass-flow ratio of 0.74. Correspondingly, the kinetic-energy efficiency varied from about 0.90 to 0.92. A larger bleed gap (0.25 in.) reduced slightly both mass flow and recovery. With no bleed, the maximum recovery level was only about 0.19 with considerably less stable subcritical range.

Airflow patterns for this axisymmetric external-compression inlet are shown in the schlieren photographs of figure 3. Both a supercritical and a subcritical minimum-stable-mass-flow operating condition are illustrated. During supercritical operation (fig. 3(a)), the compression field generated by the contoured spike appears to focus just slightly ahead of the cowl lip, thus, indicating a small amount of spillage. The combined spillage at the lip and through the internal bleed system was 0.07 of the maximum possible mass-flow rate into the inlet. At the subcritical minimum-stable-mass-flow condition (fig. 3(b)), an asymmetric bow shock moved out ahead of the cowl lip. For this condition, the combined spillage has been increased to 0.26 of the maximum possible mass-flow rate into the inlet.

For this inlet configuration, the discharge Mach numbers were quite low (0.1 or less). However, at the strut rake station, 7.13 inches downstream of the cowl lip, no evidence of flow separation was apparent for recovery levels near critical.

Two-Dimensional External-Internal-Compression Inlet

In figure 2(b), the diffuser performance characteristics are presented for the two-dimensional inlet with both sharp swept and rectangular sideplates. Inlet starting was readily accomplished by means of the variable-geometry bypass door. With the swept sideplates, a maximum, and also critical, pressure recovery of 0.41 was realized at a mass-flow ratio of 0.94. This recovery corresponds to a kinetic-energy efficiency η_{KE} of 0.94. With the rectangular sideplates, both critical recovery and mass-flow ratio were decreased by 0.04. This, presumably, was the result of flow separation on the sideplates along the line of interaction between the external-compression shocks and the sidewall boundary layers. Evidence of this separation could be detected in schlieren photographs.

The airflow patterns are shown in figure 4 for the two-dimensional external-internal-compression inlet with swept and rectangular sideplates during supercritical operation. In the first photograph (fig. 4(a)), the

inlet with the original ramp contour has the shock wave from the initial
ramp falling considerably ahead of the cowl lip with a resulting total
spillage of 0.11 of the maximum possible capture mass-flow rate m_0. With
the modified ramp contour, the initial shock wave is located closer to the
lip, and the total spillage was reduced to 0.06 of the maximum possible
mass-flow rate into the inlet.

The prime purpose of using rectangular sideplates in this study was
to obtain internal flow visualization in the area around the throat. The
results are shown in figure 4(c) and (d) for critical and supercritical
operating conditions, respectively. Note that, even at the critical con-
dition, the terminal-shock system has remained a considerable distance
downstream of the throat or design position. Presumably, shock - boundary-
layer interaction prevents further movement upstream without choking the
duct and causing shock expulsion from the inlet. The lower photograph
(fig. 4(d)) shows the relatively thick boundary layer entering the inlet
along the external-compression ramp. An adequate boundary-layer-removal
system in the vicinity of the throat (similar to that of ref. 3) might
well yield significant performance gains. In general, the theoretical
shock structure has been duplicated rather closely, insofar as focusing
the compression is concerned. The initial shock off the ramp leading
edge, however, missed the lip by a small amount, thereby causing some
attendant flow spillage.

The total-pressure distribution across the throat center span posi-
tion is presented in figure 5 for the two-dimensional inlet with its
original ramp contour. For comparison, the theoretical recovery of 0.60
(which is based solely on shock losses) is also indicated. Experimentally,
a maximum value of 0.58 and an average of about 0.51 was obtained. The
difference between this value and the maximum over-all recovery (0.41) is
attributed to friction, separation and mixing losses, and the terminal
shock being located downstream of the throat at a greater-than-design
Mach number.

In figure 6, total-pressure contour maps at the diffuser exit are
shown for the critical and a supercritical operating condition. At
critical (fig. 6(a)), the flow pattern appears generally symmetrical about
the vertical centerline with the high-energy air tending towards the upper
portion of the duct. Some separated flow accummulated in the corners.
Supercritically (fig. 6(b)), a lobe of high-energy air was formed on either
side of the centerline and was located in the upper half of the duct. Low-
energy, or separated flow, appears to have piled up in the corners and at
the center span position along the lower duct wall.

SUMMARY OF RESULTS

An experimental investigation was made to determine the diffuser
characteristics at Mach 4.95 of two separate and distinct inlet config-
urations, namely, (a) an axisymmetric fixed-geometry external-compression

inlet with a cylindrical cowl and a subsonic dump diffuser and (b) a two-dimensional external-internal-compression inlet with a variable throat bypass for starting. The following results were obtained:

1. With the axisymmetric external-compression inlet, a critical pressure recovery of 0.25 and a maximum recovery of 0.31 were obtained at mass-flow ratios of 0.93 and 0.74, respectively. A flush rearward-facing boundary-layer bleed gap in the throat was employed on this con-figuration. Without bleed, the maximum recovery was only 0.19.

2. With the two-dimensional external-internal-compression inlet, a maximum and critical recovery of 0.41 was attained with a corresponding mass-flow ratio of 0.94. A variable bypass door ahead of the throat satisfactorily handled the inlet starting problems.

Lewis Research Center
    National Aeronautics and Space Administration
   Cleveland, Ohio, September 23, 1958

REFERENCES

1. Connors, James F., and Allen, John L.: Survey of Supersonic Inlets
    for High Mach Number Applications. NACA RM E58A20, 1958.

2. Connors, James F., and Anderson, Leverett A., Jr.: A Two-Dimensional
    External-Internal-Compression Inlet with Throat Bypass at Mach 3.05.
    NASA MEMO 10-3-58E, 1958.

3. Connors, James F., and Flaherty, Richard J.: High Mach Number, Low-
    Cowl-Drag, External-Compression Inlet with Subsonic Dump Diffuser.
    NACA RM E58A09, 1958.

8

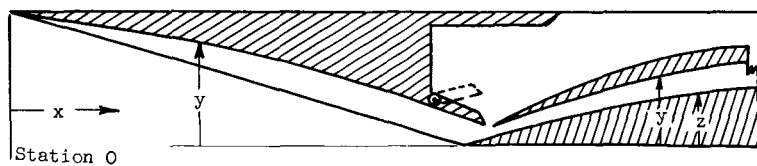TABLE I. - DIMENSIONAL DETAILS FOR AXISYMMETRIC EXTERNAL-COMPRESSION INLET
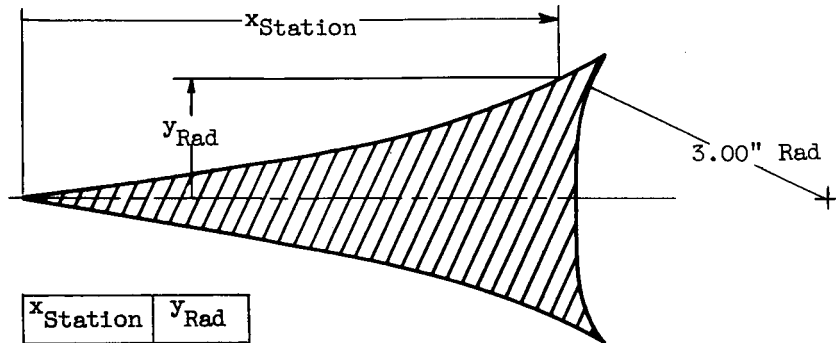
$x_{Station}$	y_{Rad}
0	0
2.000	.282
3.000	.430
4.000	.592
5.000	.778
6.000	.987
7.000	1.232
7.750	1.454
8.250	1.639
8.500	1.742
8.750	1.867
9.285	2.200

(a) Spike.
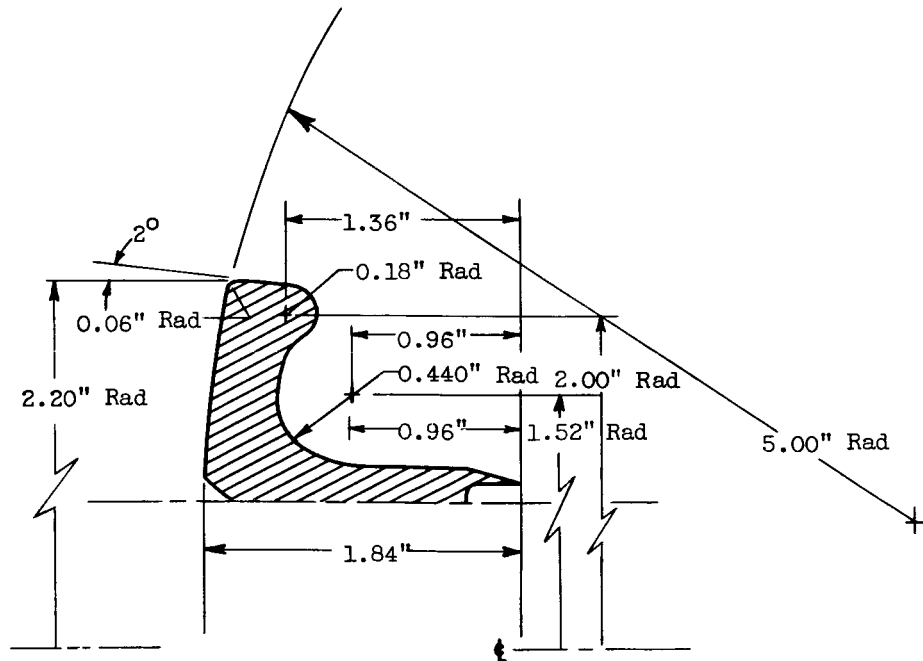
(b) Subsonic-dump section.

E-123

QL-2

TABLE II. - DIMENSIONAL DETAILS FOR TWO-DIMENSIONAL

EXTERNAL-INTERNAL-COMPRESSION INLET

x	y^a	y^b	z
0	5.0	5.0	-----
3.32	(c)	4.54	-----
4.50	(c)	4.362	-----
5.50	(c)	4.192	-----
6.00	4.05	-----	-----
6.50	3.966	4.063	-----
7.00	3.880	3.917	-----
7.50	3.790	3.818	-----
8.00	3.694	3.710	-----
8.50	3.590	3.594	-----
9.00	3.476	3.476	-----
9.50	3.352	3.352	-----
10.00	3.220	3.220	-----
10.50	3.080	3.080	-----
10.85	2.980	2.980	-----
15.32	(c)	(c)	0.00
15.61	1.534	1.534	-----
16.70	-----	-----	.010
17.00	-----	-----	.034
17.25	-----	-----	.068
17.50	-----	-----	.122
17.61	-----	-----	.154
18.10	0.759	0.759	-----
18.23	-----	-----	.349
18.50	0.880	0.880	.428
19.00	1.042	1.042	.518
19.50	1.210	1.210	.720
20.00	1.380	1.380	.860
20.50	1.540	1.540	.994
21.00	1.710	1.710	1.120
21.50	1.864	1.864	1.238
22.00	2.020	2.020	1.344
22.50	2.160	2.160	1.446
23.00	2.304	2.304	1.542
23.50	2.440	2.440	1.622
24.00	2.564	2.564	1.698
24.50	2.680	2.680	1.760
25.00	2.788	2.788	1.818
25.50	2.880	2.880	1.860
26.00	2.956	2.956	1.900
26.50	3.010	3.010	1.930
27.00	3.040	3.040	1.950
27.18	3.045	3.045	1.955
27.50	3.045	3.045	1.955

[a]Original ramp contour.

[b]Modified ramp contour.

[c]Straight taper.

Movable
exit plug

18.875"

9.21"

4.75"

2" Sting

0.25" Bleed
gap

(a) Axisymmetric external-compression inlet with cylindrical cowl and subsonic dump.

Movable
wedge

CD-6352

Bypass

Variable
bypass
door

Swept sideplates

Rectangular sideplates
with glass inserts

Lip   Throat   Compressor face
15.38" 18.25"   27.50"

Station 0

Max. capture
streamtube

5"

5"
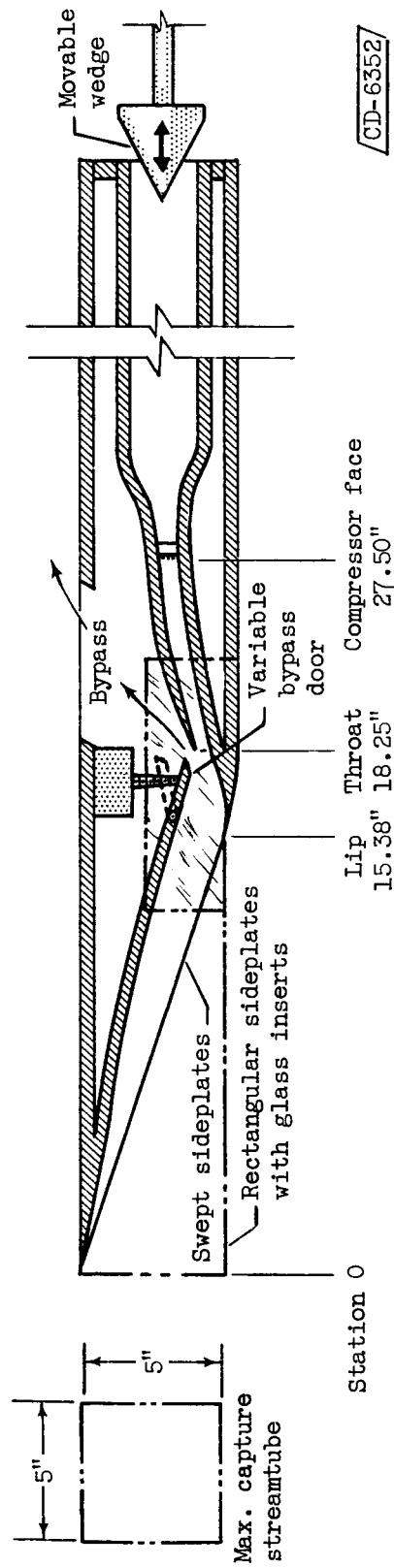
(b) Two-dimensional external-internal-compression inlet with variable throat bypass.

Figure 1. - Experimental apparatus.

E-123

E-123

CL-2 back

Actuator

Bypass

M = 0.617
λ = 17.45°

CD-6353

M = 3.46
λ = 16.9°

M = 1.8
λ = 17.45°

M = 2.46
λ = 0

M = 4.0
λ = 9°

M₀ = 4.95
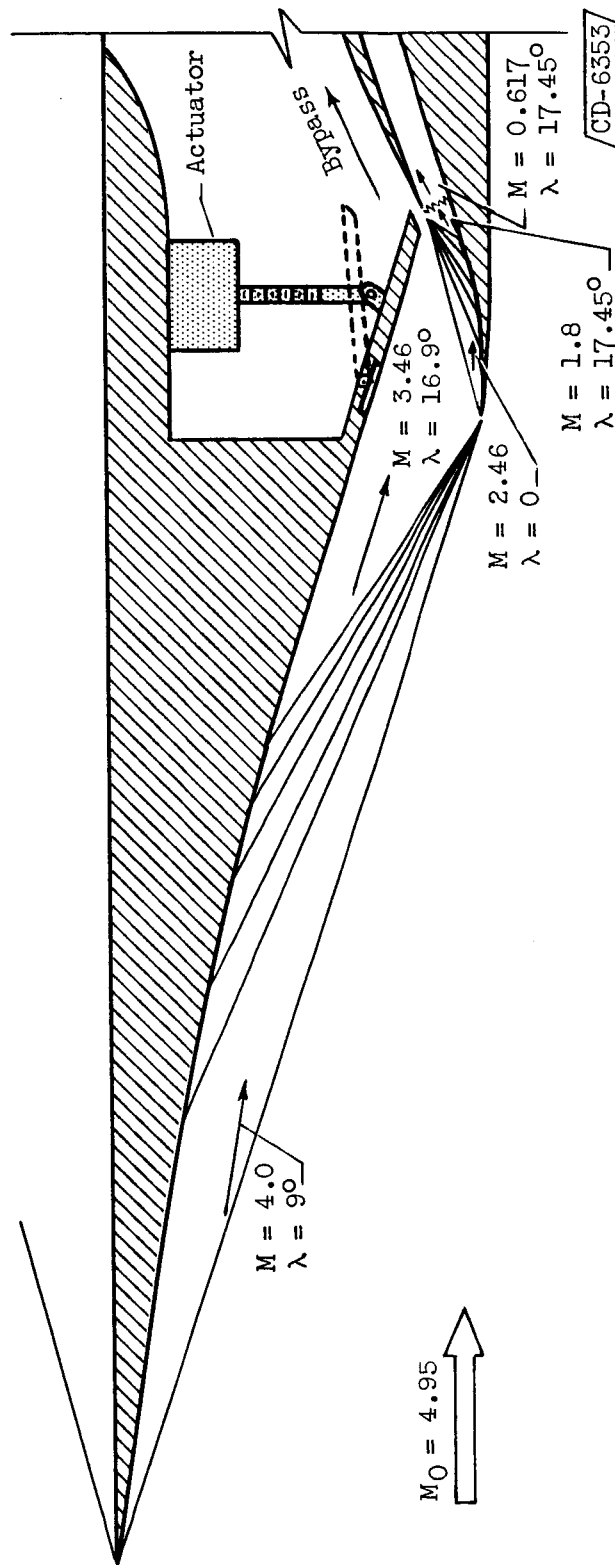
(c) Theoretical shock patterns for the two-dimensional external-internal-compression inlet; theoretical total-pressure recovery, 0.60.

Figure 1. – Continued. Experimental apparatus.

C-47925
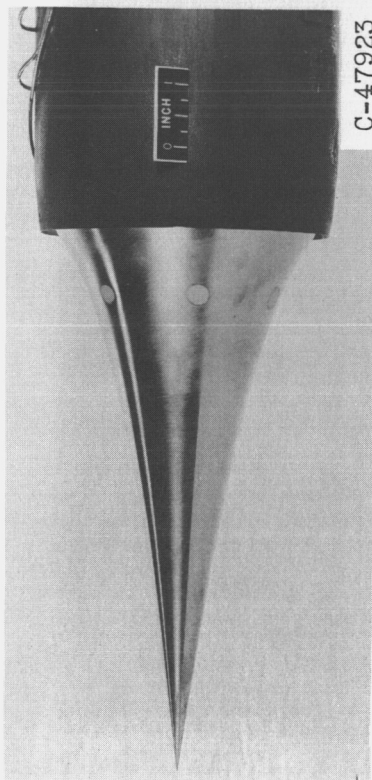
Cowl removed

(d) Axisymmetric external-compression inlet.

C-47921

Rectangular sideplates

C-47923

Cowl in position
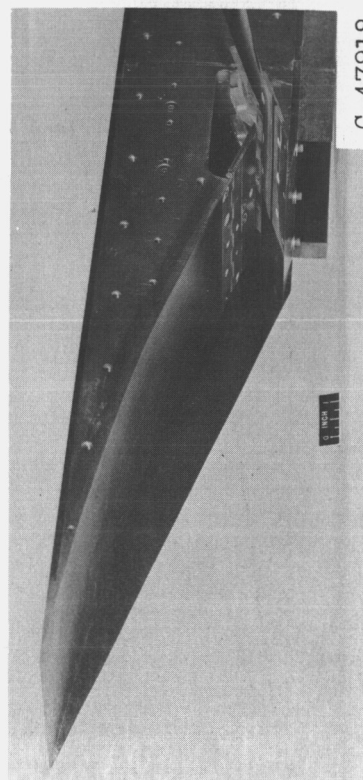
C-47918

Swept sideplate, near plate removed
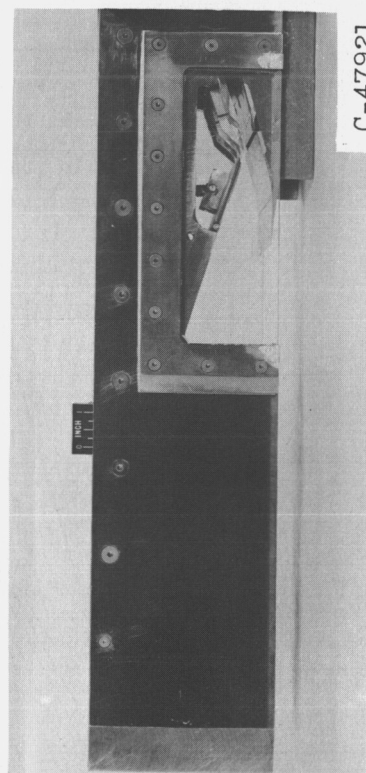
(e) Two-dimensional external-internal-compression inlet.

Figure 1. - Concluded. Experimental apparatus.

E-123

(a) Axisymmetric external-compression inlet with cylindrical cowl and subsonic dump.

(b) Two-dimensional external-internal-compression inlet with variable throat bypass, modified ramp contour.
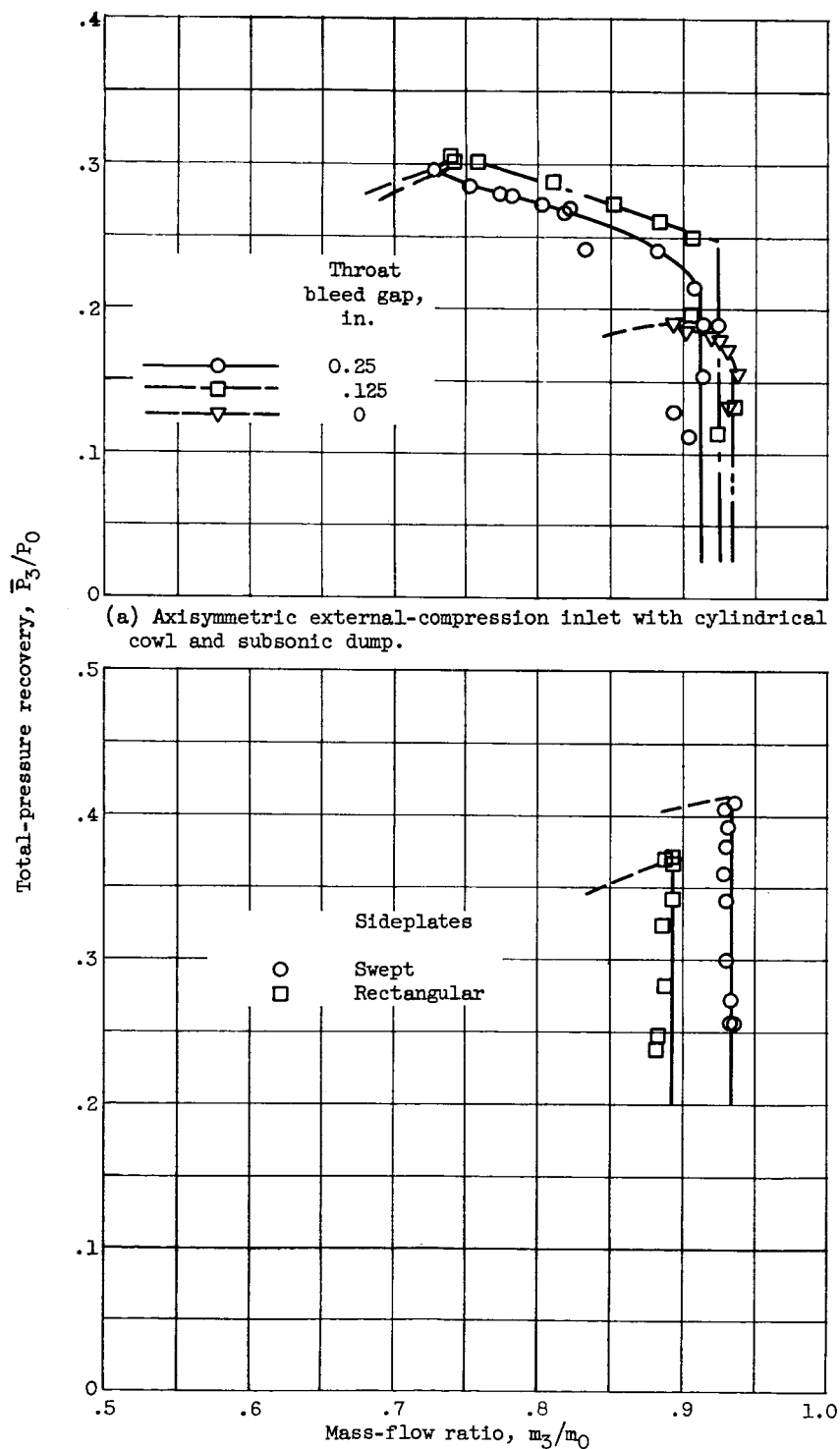
Figure 2. - Diffuser performance characteristics at Mach number 4.95.
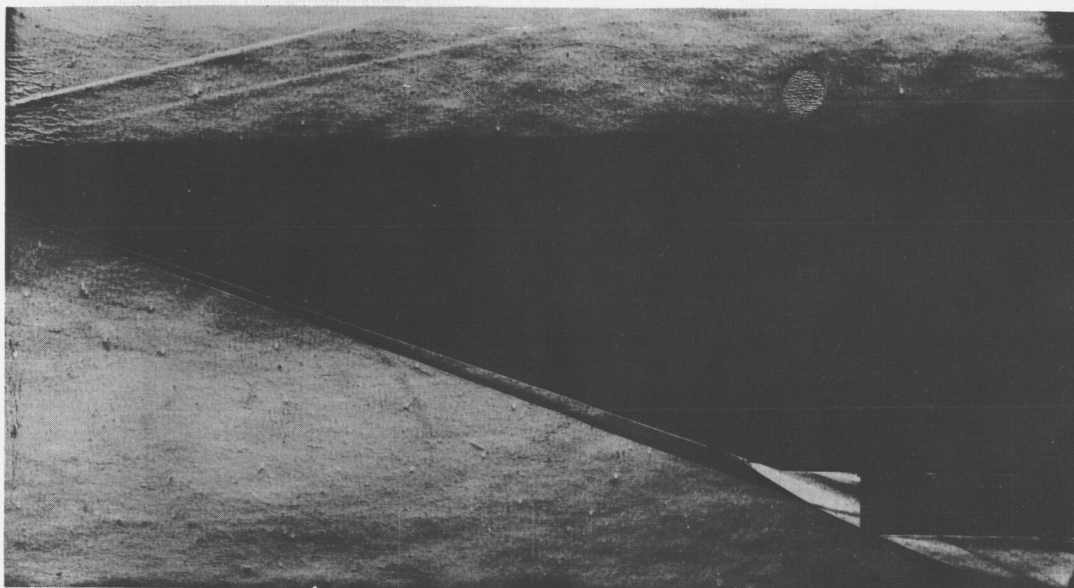
(a) Supercritical operation.

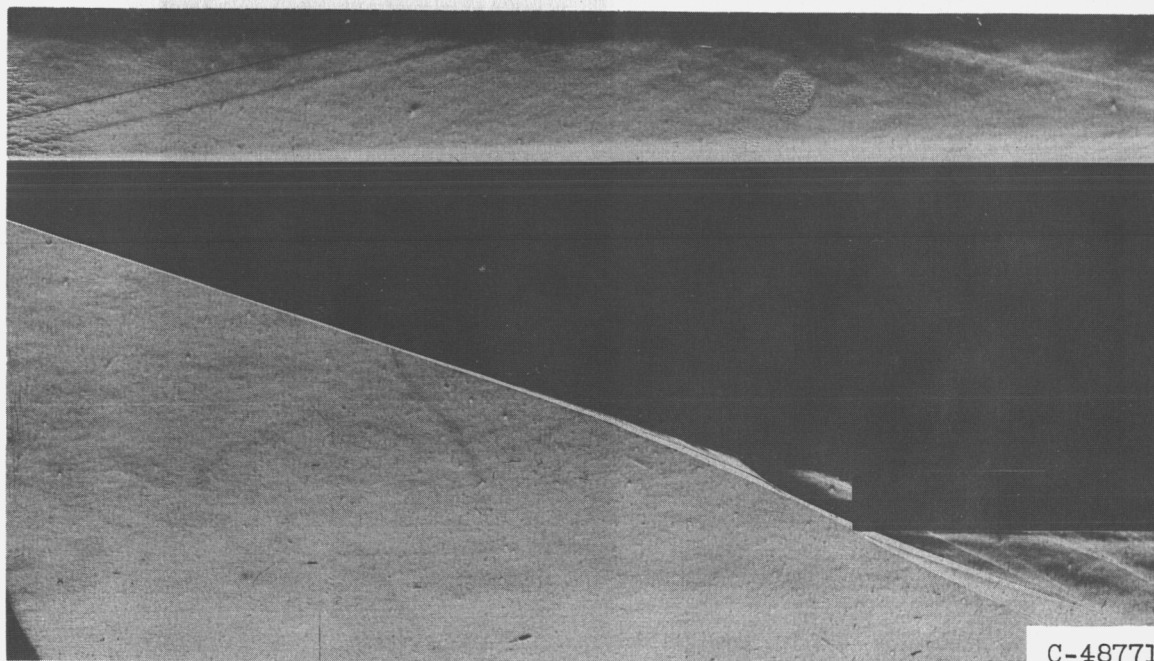C-48769
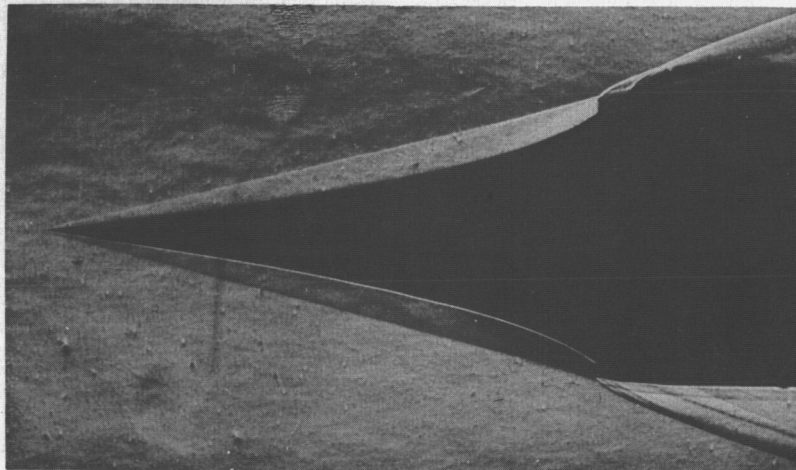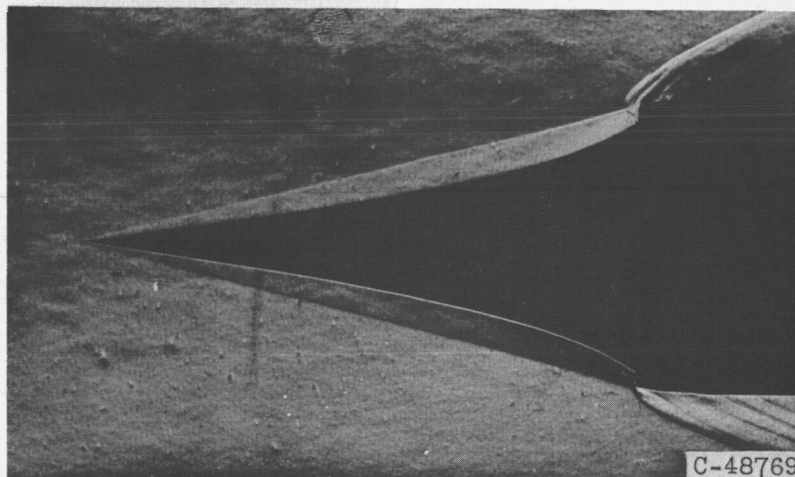
(b) Subcritical, minimum-stable-mass-flow operation.

Figure 3. - Airflow patterns for axisymmetric external-
compression inlet with cylindrical cowl and subsonic
dump; Mach 4.95.

(a) Swept sideplates, original ramp contours, supercritical operation.
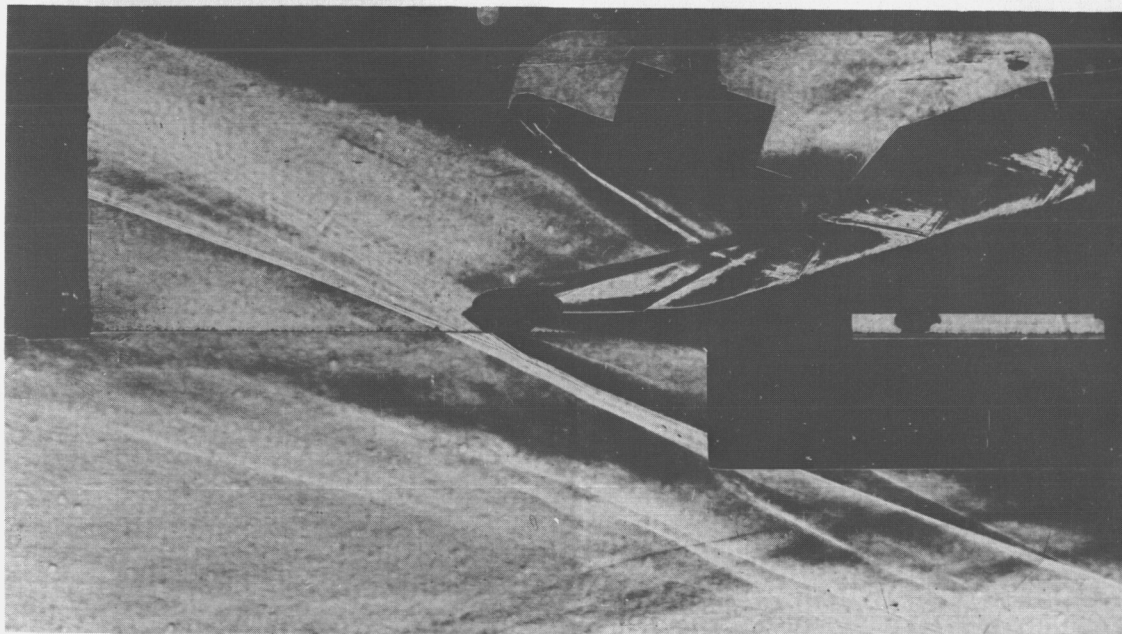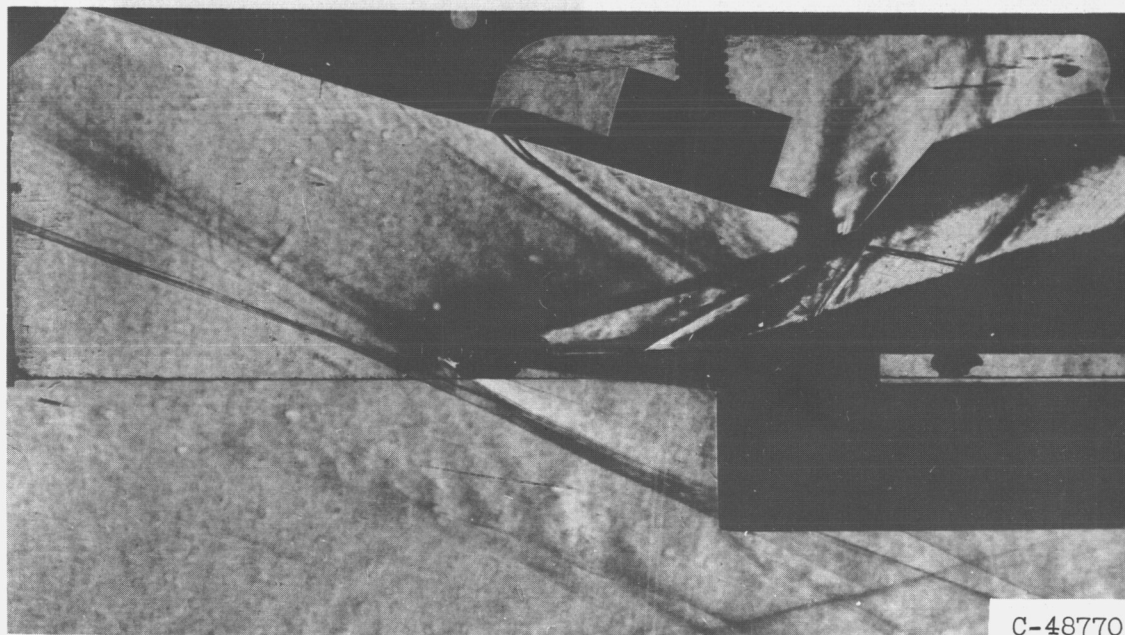

C-48771

(b) Swept sideplates, modified ramp contour, supercritical operation.

Figure 4. - Airflow patterns for two-dimensional external-internal-compression inlet with variable throat bypass; Mach 4.95.

E-123

(c) Rectangular glass sideplates, modified ramp contour, critical operation.

C-48770

(d) Rectangular glass sideplates, modified ramp contour, super-critical operation.

Figure 4. - Concluded. Airflow patterns for two-dimensional external-internal-compression inlet with variable throat bypass; Mach 4.95.
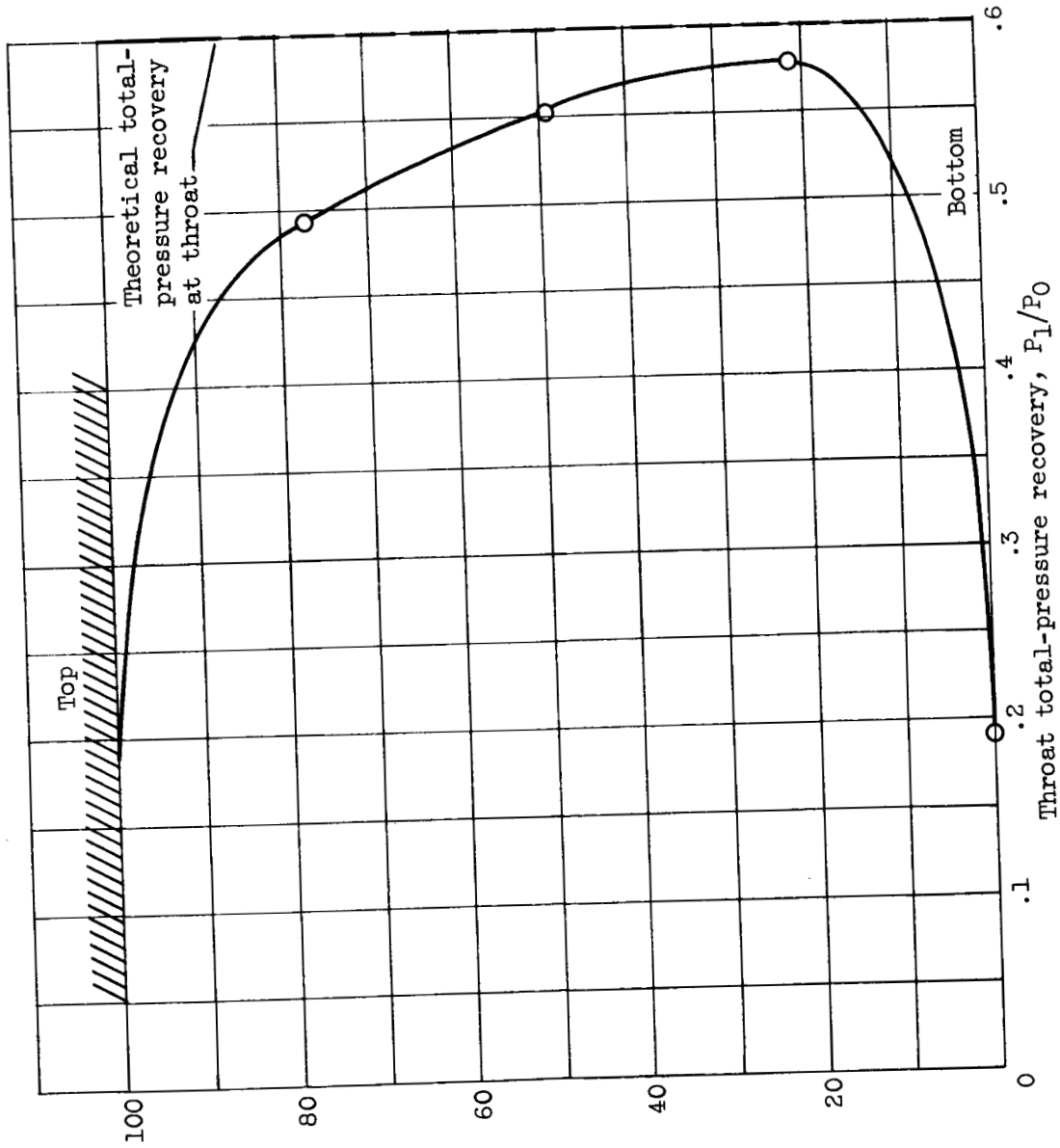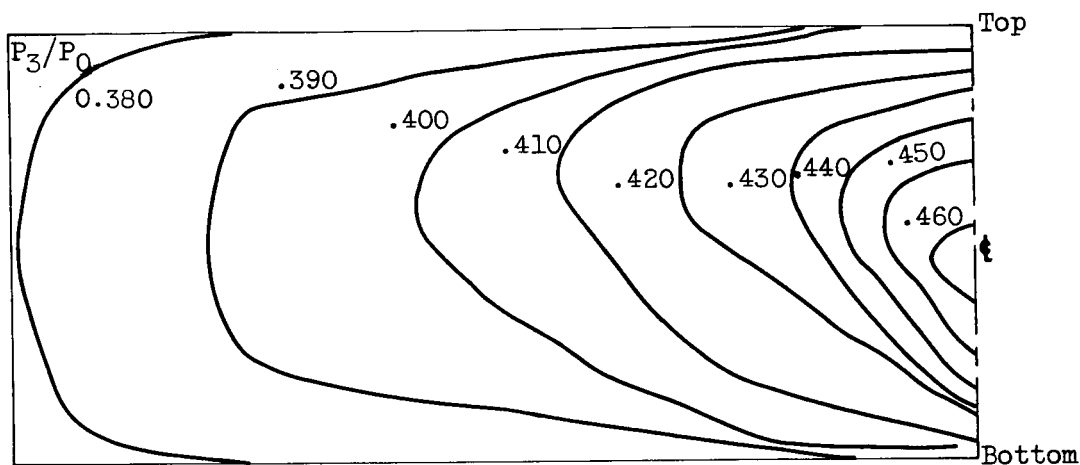
E-123

Figure 5. - Total-pressure profile across throat centerspan position for the two-dimensional inlet with the original ramp contours; Mach 4.95.

Throat total-pressure recovery, P_1/P_0

Distance from wall, percent of total throat height

Theoretical total-pressure recovery at throat

Top

Bottom

Top

P_3/P_0

0.380 .390 .400 .410 .420 .430 .440 .450 .460

¢

Bottom

(a) Critical operation; total-pressure recovery, 0.411; mass-
flow ratio, 0.936; ratio of local static to free-stream
total pressure, 0.381.

Top

P_3/P_0

0.350
.340
.330 .320 .310
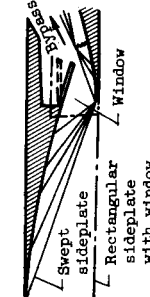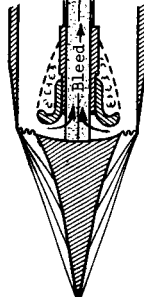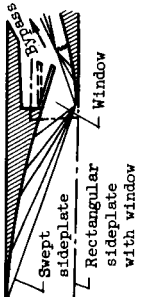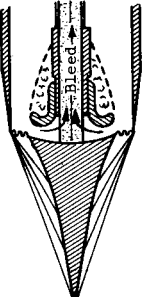.300 .290
.280
.270

¢

Bottom
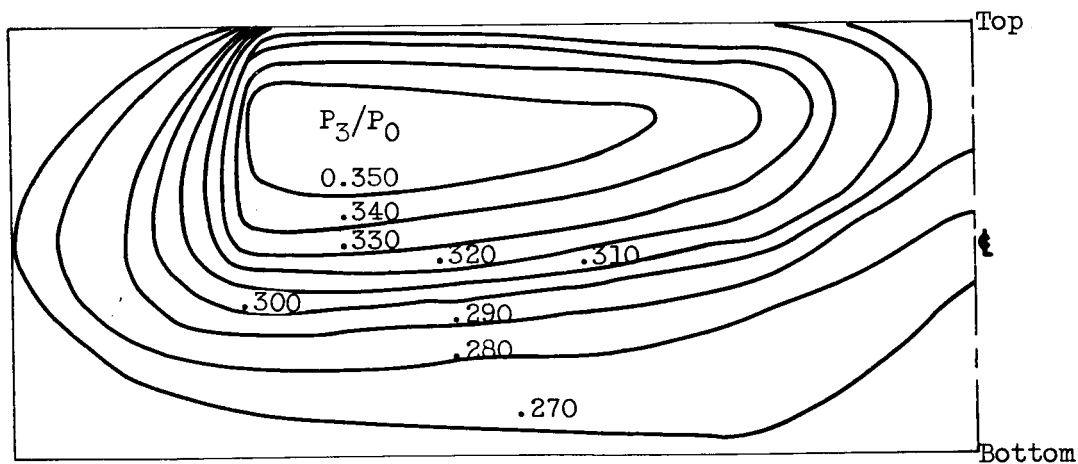
(b) Supercritical operation; total-pressure recovery, 0.301;
mass-flow ratio, 0.929; ratio of local static to free-stream
total pressure, 0.269.

Figure 6. - Total-pressure contours at the diffuser exit for the
two-dimensional inlet; Mach 4.95.

NOTES: (1) Reynolds number is based on the diameter of a circle with the same area as that of the capture area of the inlet.

(2) The symbol * denotes the occurrence of buzz.

INLET BIBLIOGRAPHY SHEET

Report and facility	Description			Test parameters				Test data				Performance		Remarks
	Configuration	Number of oblique shocks	Type of boundary-layer control	Free-stream Mach number	Reynolds number × 10⁻⁶	Angle of attack, deg	Angle of yaw, deg	Drag	Inlet-flow profile	Discharge-flow profile	Flow picture	Maximum total-pressure recovery	Mass-flow ratio	
CONFID. NASA MEMO 12-18-58E Lewis 1-by 1-foot wind tunnel	Swept sideplate / Rectangular sideplate with window / Bypass / Window	Isentropic	Bypass and flush slot ahead of throat. Ram scoop in throat.	4.95	2.68	0	0	---	✓	✓	✓	0.41	0.94	Kinetic-energy efficiency, $\eta_{K.E.} = 0.94$
CONFID. NASA MEMO 12-18-58E Lewis 1-by 1-foot wind tunnel	Bleed	Isentropic	Variable flush annular slot at throat.	4.95	2.26	0	0	---	---	---	✓	0.31 .25 .19	0.74 .93 .97	Bleed gap = 0.125 in. with 0.31 recovery. No bleed with 0.19 recovery and reduced stable subcritical range. $\eta_{K.E.} = 0.90$ 0.92
CONFID. NASA MEMO 12-18-58E Lewis 1-by 1-foot wind tunnel	Swept sideplate / Rectangular sideplate with window / Bypass / Window	Isentropic	Bypass and flush slot ahead of throat. Ram scoop in throat.	4.95	2.68	0	0	---	✓	✓	✓	0.41	0.94	Kinetic-energy efficiency, $\eta_{K.E.} = 0.94$
CONFID. NASA MEMO 12-18-58E Lewis 1-by 1-foot wind tunnel	Bleed	Isentropic	Variable flush annular slot at throat.	4.95	2.26	0	0	---	---	---	✓	0.31 .25 .19	0.74 .93 .97	Bleed gap = 0.125 in. with 0.31 recovery. No bleed with 0.19 recovery and reduced stable subcritical range. $\eta_{K.E.} = 0.90 - 0.92$

NACA-C-8070(2-13-58)

Bibliography

These strips are provided for the convenience of the reader and can be removed from this report to compile a bibliography of NACA inlet reports. This page is being added only to inlet reports and is on a trial basis.